Particle & Particle Systems Characterization
www.particle-journal.com

Magnetic Field-Controlled Release of Paclitaxel Drug from Functionalized Magnetoelectric Nanoparticles

*Rakesh Guduru and Sakhrat Khizroev**

Using magnetoelectric nanoparticles (MENs) for targeted drug delivery and on-demand, field-controlled release can overcome the control challenges of the conventional delivery approaches. The magnetoelectric effect provides a new way to use an external magnetic field to remotely control the intrinsic electric fields that govern the binding forces between the functionalized surface of the MEN and the drug load. Here, a study is reported in which the composition of the intermediate functionalized layer is tailored to control not only the toxicity of the new nanoparticles but also the threshold magnetic field for the dissociation of the drug from 30-nm $CoFe_2O_4$–$BaTiO_3$ core–shell MENs in a controllably wide field range, from below 10 to over 200 Oe, as required to facilitate superficial, intermediate, and deep-tissue drug delivery. Paclitaxel is used as a test drug. Specific experiments are described to maintain low toxicity levels and to achieve controllable dissociation of the drug molecules from the MENs' surface at three different subranges—low (<10 Oe), moderate (100 Oe), and high (>200 Oe)—by selecting the following 2-nm intermediate layers: i) glycerol monooleate (GMO), ii) Tween-20, and iii) ethyl-3-(3-dimethylaminopropyl)carbodiimide (EDC). Field-dependent FTIR, absorption spectra, atomic force microscopy, magnetometry analysis, zeta-potential measurements, and blood circulation experiments are used to study the described functionalization effects.

1. Introduction

Over the last decade, nanostructures have been widely used to deliver therapeutics drugs to the diseased tissue in order to increase the bioavailability and reduce toxic side effects to the healthy tissues in the same microenvironment.[1–3] Using surface modification to further tailor important characteristics of the nanostructures is a promising approach to the development of next-generation applications in medicine, biology, and biotechnology.[4–7] In the field of drug delivery, the surface modification of nanostructures has a crucial role in determining drug binding and release kinetics.[8,9] Commonly used surface-functionalizing agents for coating nanostructures include copolymer poly(lactic-*co*-glycolic acid) (PLGA), non-ionic surfactant of oil soluble/dispersible-type glycerol monooleate (GMO), small natural homopolymer poly-L-lysine, polysorbate surfactant Tween-20, and water-soluble ethyl-3-(3-dimethylaminopropyl)carbodiimide (EDC).[10–14] For example, the main reason for using non-ionic surfactants (GMO and Tween-20) would be to achieve a noncovalent interaction between the drug cargo and the intermediate layer.[12,15] Because the non-covalent interaction is relatively weak, it is possible to use a relatively low magnetic field with these surfactants to control the binding affinity between the drug and the nanoparticle and consequently to trigger almost 100% release of the bound drug on demand. By contrast, the reason for using the EDC cross-linker would be to achieve a relatively strong covalent binding between the drug cargo and the intermediate layer (carbodiimide group) and consequently ensure that only a relatively large field could trigger the release on demand. As a carbodiimide, EDC reacts with various forms of amides and hydroxyl functional groups.[16] The mechanisms of drug delivery and release using most of these surface-functionalized nanostructures are typically governed by the change in pathological conditions, such as pH, temperature, redox microenvironments, and enzymatic reactions.[17–20] Consequently, the capability to control delivery and particularly release processes in a wide range of properties, specifically suited for different applications, remains an important challenge. Recently, we showed that alternatively it is possible to exploit the magnetoelectric (ME) effect in magnetoelectric nanoparticles (MENs) to release the therapeutic drug cargo via application of a low-energy magnetic field without compromising the structural and functional integrity of the drug at body temperature.[21–24] The ME effect provides a physical mechanism to use an external magnetic field for remote access of the intrinsic electric fields that govern the binding forces between the surface of the MEN and the drug load. The capability to remotely control this binding force would be an important milestone in the development of nanostructures for controlled targeted drug delivery and release. Previously, we have shown that there is a certain frequency-dependent magnetic field threshold for the drug to be released. Hereafter, we

M.S. R. Guduru, Prof. S. Khizroev
Department of Electrical and Computer Engineering
College of Engineering
Florida International University
Miami, FL 33174, USA
E-mail: khizroev@fiu.edu
M.S. R. Guduru, Prof. S. Khizroev
Herbert Wertheim College of Medicine
Florida International University
Miami, FL 33174, USA

DOI: 10.1002/ppsc.201300238

refer to this field as the dissociation field. This field is determined by the ionic and/or covalent interaction between the two bonded entities, i.e., the oppositely charged MEN and drug molecule in the bond (polarized due to the chemical interaction). This dissociation field can be strongly influenced by a thin (≈2 nm) intermediate layer, which modifies or modulates the polarization of the two entities. Therefore, we refer to this intermediate layer as the functional layer. The important goal of the study is to demonstrate how tailoring the composition of the intermediate layer can be used to control the dissociation field magnitude and frequency values, which are specific for each application. In particular, this study aims to explore functional-layer materials that could provide the dissociation field in these three practical regions: i) low (<10 Oe), ii) moderate (100 Oe), and iii) high (>200 Oe) at a frequency range from 0 to over 1000 Hz. These field regions are relevant for many important applications, e.g., treatment of HIV in the brain, remote magnetic field-controlled stimulation of selective regions in the central nervous system (CNS), deep-tissue drug delivery for cancer treatment, contrast-enhanced high-sensitivity magnetic imaging, and others. Furthermore, control by the field frequency provides an additional advantage that is particularly important for the release process.[21] Introducing the intermediate functionalization layer will result in changing the binding affinity between the drug and the surface of the MEN. One important requirement of this layer is for it to maintain sufficiently strong binding with the surface of the MEN while keeping binding to the drug molecules sufficiently weak. Accordingly, we implement this concept by studying the following three intermediate layers: (i) GMO, (ii) Tween-20, and (iii) EDC. In this study, we use Paclitaxel (PTX or Taxol) as the model drug as it is one of the most widely used antineoplastic agents against ovarian, breast, neck, head, and non-small-cell lung carcinoma, as well as others.[25–27] We use $CoFe_2O_4$–$BaTiO_3$ coreshell MENs as a drug delivery vehicle, owing to their ability to exhibit magnetoelectric effect at body temperature and because they represent one of the most widely studied MEN systems.[28,29] Finally, it should be mentioned that because of its fundamental nature the discussed approach can be applied to many other drugs besides Paclitaxel.

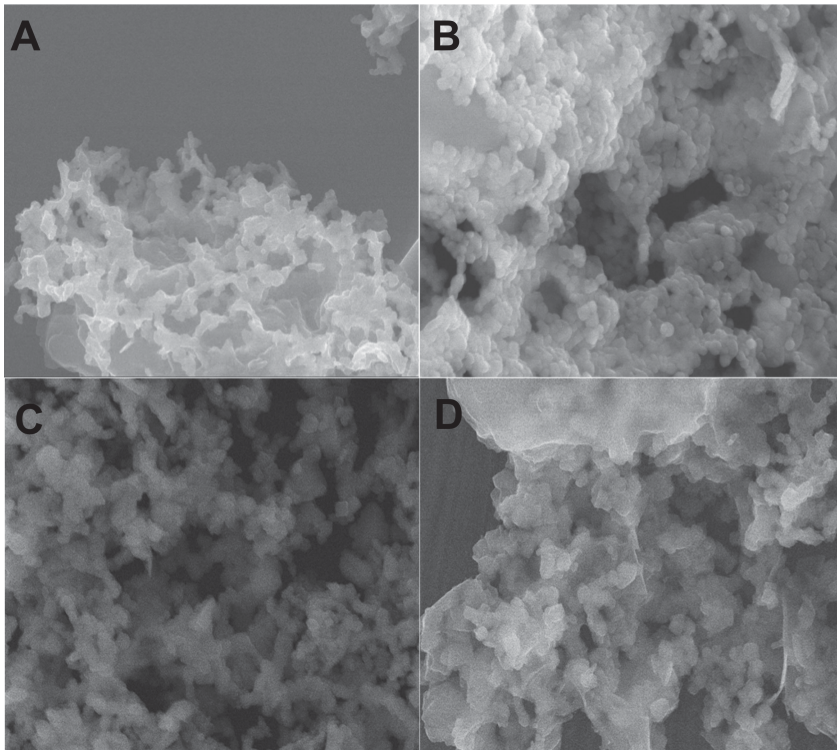

Figure 1. SEM image showing of the MENs. A) Uncoated MENs, B) GMO-MENs, C) Tween20-MENs, and D) EDC-MENs. Scale bar = 100 nm.

2. Results

2.1. Intermediate (Functionalization) Layer on the MEN

As mentioned above, in order to tailor the dissociation field magnitude and frequency required to trigger the release of the bonded PTX from MENs in a specific application, we coated the surface of the MEN with the following three intermediate layers: GMO, Tween-20, and EDC, respectively, as shown in the **Figure 1**. By its nature, zeta potential indirectly reflects the binding affinity between a nanomaterial and the drug. To some degree of approximation, in the case of nanoparticles, the higher zeta potential implies the higher effective charge and therefore results in the higher Coulomb force and the higher dissociation field.[30] We measured the surface zeta potential, size, and Fourier transform infrared (FTIR) absorption spectrum of MENs before and after functionalization to understand the effects of the selected surface modification. As summarized in **Table 1**, the results show a dependence of the zeta-potential values on

Table 1. Change in zeta potential and size measurements of the MENs surface before and after surface functionalization. Zeta-potential values are the average and standard deviation of three independent trails ($n = 3$).

Functionalizing agent	Size [nm][a)]	Zeta potential [mV][a)]
Uncoated-MENs	28.6 ± 7.5	–45.0 ± 1.72
GMO-MENs	30.9 ± 8.6	–41.6 ± 0.26
Tween-20-MENs	29.5 ± 5.6	–34.9 ± 0.20
EDC-MENs	31.1 ± 4.4	–30.4 ± 0.81
PTX-MENs	28.9 ± 7.7	–44.8 ± 1.67
PTX-GMO-MENs	44 ± 6.6	–40.7 ± 0.1
PTX-Tween20-MENs	32.3 ± 6.1	–31.1 ± 0.51
PTX-EDC-MENs	33.8 ± 3.2	–27.7 ± 1.3

[a)]Average ± standard deviation.

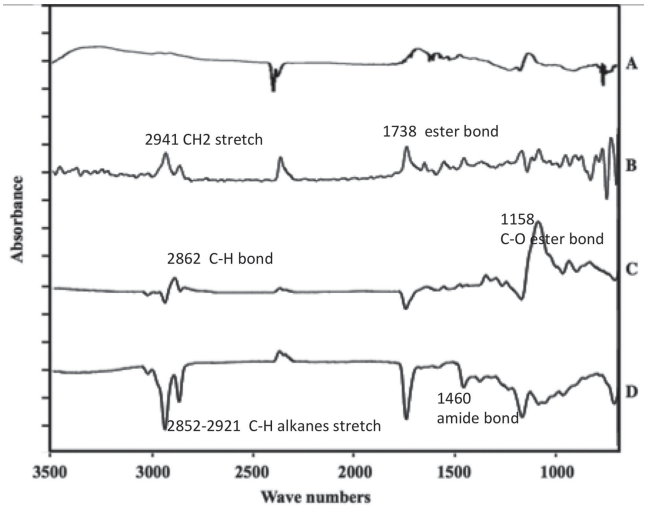

Figure 2. FTIR for surface-functionalized MENs. A) MENs, B) GMO-MENs, C) Tween-20-MENs, and D) EDC-MENs.

the type of functional material used (average of three independent measurements): –45.0 mV ± 1.72 for nonfunctionalized MENs, –41.6 mV ± 0.26 for GMO-MENs, –34.9 mV ± 0.20 for Tween-20-MEN, and –30.4 mV ± 0.81 for EDC-MENs. The results also indicate a slight (≈3%) increase in the average size (n = 3) of MENs after coating with the functionalization layer: 28.6 nm ± 7.5 for MENs, 30.9 nm ± 8.9 for GMO-modified MENs, 29.5 nm ± 5.6 for Tween-20-modified MENs, and 31.1 nm ± 4.4 for EDC-modified MENs. FTIR spectrum of the GMO-modified MEN surface (**Figure 2**B) shows peaks at 1738 and 2941 cm^{-1}, which correspond to the ester bond and CH_2 stretching modes, respectively. The peaks indicate the presence of the GMO layer on the surface of the MEN.[12] The Tween-20-modified MEN surface (Figure 2C) displays FTIR peaks at 1158 and 2862 cm^{-1} that correspond to C–O ester bonds and C–H bonds, respectively.[31] Figure 2D shows FTIR spectral peaks of the EDC-modified MENs at 2852 to 2921 cm^{-1} and 1460 cm^{-1}, which correspond to C–H alkanes stretch and the amide bonds, respectively.[32]

2.2. PTX Drug Loading onto MEN Surface

PTX drug loading onto differently functionalized MEN surfaces was achieved by incubating the drug with the MENs in PBS buffer (pH 7.2). Time-dependent drug-binding kinetics was performed to determine the ideal incubation time to maximize the drug-loading percentage. The knowledge of the loading capability of the nanocarrier (MENs) is important for optimizing its drug delivery characteristics. **Figure 3**A shows that ≈16%, ≈42%, ≈91%, and ≈77% of PTX binds to the uncoated MENs, GMO-MENs, Tween20-MENs, and EDC-MENs, respectively, in 3 h of incubation. The drug-loading percentage was determined by measuring the UV light absorption maxima at 230 nm in the supernatant solution. Figure S4 (Supporting Information) shows the PTX absorption maxima at different drug concentrations. To determine the binding efficacy of the PTX drug with different MENs, we performed a binding isotherm study by varying the drug concentration from 25 to 200 μg mL^{-1} per 1 mg of MENs. As shown in Figure 3B, the results indicate that the PTX binding efficacy has the highest value for EDC-MENs (79–86 μg), followed by Tween20-MENs (55–58 μg), GMO-MENs (34–39 μg), and the uncoated MENs (3–4 μg). To simulate the PTX binding efficacy in the human blood circulatory system, we continuously circulated these particles for 2 h using a peristaltic pump at a flow rate of 8 mL min^{-1}. The measured percentage of PTX (loaded on MENs) that remained intact as a result of the circulation experiment is 91.1% for EDC-MENs, 87.0% for Tween-20-MENs, 79.5% for GMO-MENs, and 58.4% for nonfunctionalized MENs.

2.3. On-Demand Paclitaxel Release Using Remote Magnetic Fields

PTX bound to different functionalization layers (of MENs) was treated with DC and AC magnetic fields to release the drug without affecting its functional and structural integrity, according to the procedures described in detail in our previous publication.[21] As shown in **Figure 4**, the results indicate that the threshold magnetic field and frequency required to trigger the release of over 70% of the drug from the uncoated MENs are approximately 10 Oe and 1000 Hz, respectively. For GMO-MENs, the two values for releasing over 97% of PTX are 100 Oe and 0 Hz, respectively. For Tween-20-MENs, to release over 45% of the drug, the two values are 200 Oe and 1000 Hz, respectively, whereas for EDC-MENs with the same field and frequency values, we can release barely above 5% of the drug. (Note: owing to limitations of our experimental set-up, we could not exceed field and frequency values above 200 Oe and 1000 Hz, respectively.)

2.4. In Vitro Cytotoxicity

An in vitro cytotoxicity study was performed using XTT assay to account for the cytotoxic effects of the surface-modified MENs on human ovarian cancer cells (SKOV-3). As summarized in

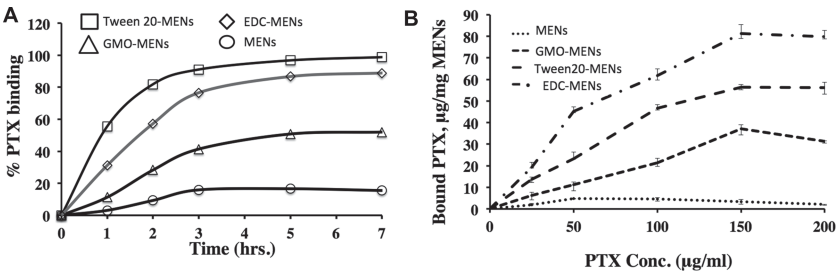

Figure 3. PTX drug loading. A) Time kinetic of PTX binding onto different MENs surface at 1:10 weight ratio (0.1 mg of PTX and 1 mg of MENs). B) Binding isotherm of PTX onto different MENs surface at varying PTX drug concentration and for 3 h incubation time.

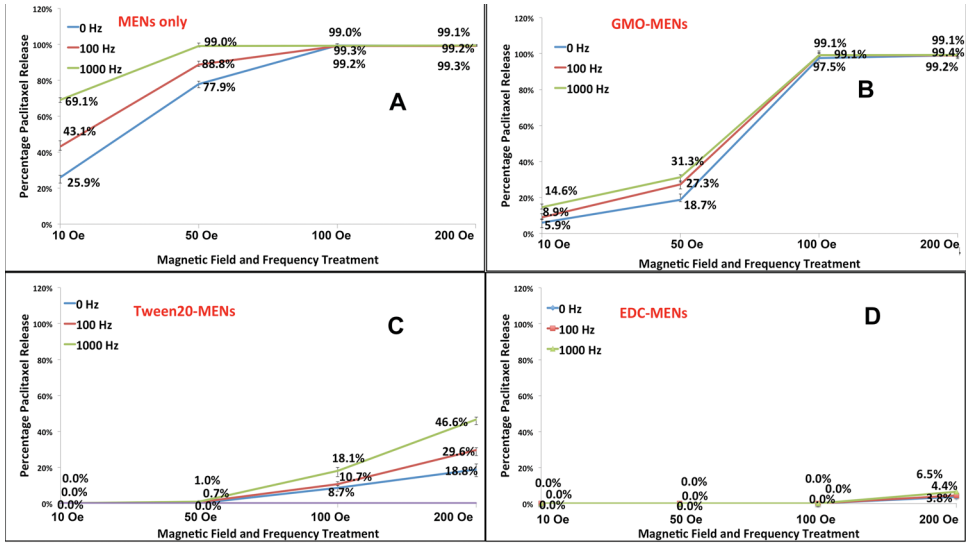

Figure 4. Magnetic field and frequency dependence of PTX drug release from functionalized MENs (A. Uncoated MENs, B. GMO-MENs, C. Tween20-MENs, and D. EDC-MENs.).

Figure 5, the results showed no significant toxicity on SKOV-3 cells when treated with MENs (≈96% cells viable), GMO-MENs (≈100% cells viable), and Tween-20-MENs (≈89% cell viable) at the highest concentration level of 50 μg mL^{-1}. However, EDC-MENs showed relatively low toxicity (≈77% cells viable) for the same concentration. As expected, GMO-MENs show no toxicity in the entire field and frequency regions under study. (Note: in vitro cytotoxicity measurements were also performed in the presence of magnetic field.) However, the results did not show any significant dependence on magnetic field.

3. Discussion

Previously, we have shown how low-energy external magnetic fields could increase the bioavailability of the therapeutic drug cargo at the site of diseased tissue using the MENs, instead of the conventional magnetic nanoparticles (MNs), as the delivery vehicle, thereby overcoming the toxic side effects caused to healthy tissue.[21,33,34] One important advantage of using MEN-based delivery is the fact that different remote magnetic field modes can be used for delivery and release of the therapeutic payloads with unprecedented energy efficiency that promises widespread medical application in the future. Exactly as with conventional MNs, the drug delivery (navigation through the body) with MENs can be achieved by a DC magnetic field gradient with a field magnitude in the range specific to the targeted region (superficial or deep-tissue). As for the release process, it cannot be achieved with the conventional MNs and can be achieved with MENs via application of either low-energy AC or relatively high DC fields. Therefore, unlike the conventional MNs, MENs offer a new capability of field-controlled release. To allow high-efficacy independent control of delivery (navigation) and/or release, MENs allow to separate the respective functions in the magnetic field magnitude and frequency domains in a broad spectrum. Furthermore, the ability to vary the control fields in the widest possible ranges (in magnitude and frequency domains) can significantly increase the range of potential applications for MENs. For example, it is known that to target deep-tissue carcinoma, a relatively high DC magnetic field (above 100 Oe) is required for the navigation. By contrast, superficial drug delivery can be achieved by field gradients with a DC field weaker than 100 Oe. Furthermore, the dependence of the release on the field frequency provides another powerful control knob. For example, for GMO-MENs at a 1000-Hz frequency, a 10-Oe field was sufficient to achieve the same release percentage as that achieved by the DC field at a higher than 100 Oe magnitude. Previously, we have shown that the MEN-triggered

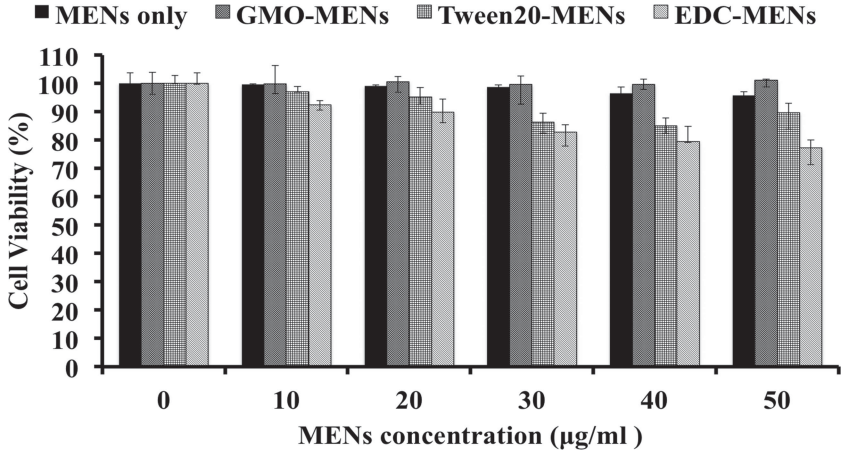

Figure 5. XTT cytotoxicity assay. Viability of the SKOV-3 cells was determined using XTT assay after treating with various concentrations of MENs (uncoated MENs, GMO-MENs, Tween-20-MENs, and EDC-MENs) for 48 h.

release depended on both the field's magnitude and frequency. In particular, we described one plausible physical concept according to which the DC field component was used for the navigation purpose (through controlling spatial field gradients), whereas the AC field component was used for the controlled drug release off the MEN-based carrier.[21] The physics of the AC-triggered release was explained through the frequency-dependent spin-initiated torque. Indeed, our current results confirm that increasing the frequency reduced the disassociation field (Figure 4). This trend is observed for all the three types of functional layer.

To control the value of the dissociation field, we varied the effective binding strength between the MEN and the drug molecule (F_{MD}). By introducing the intermediate (functionalization) layer between the MEN and the drug molecule, it is important to maintain the following inequality: $F_{MI} > F_{ID}$, where F_{MI} and F_{ID} are the binding forces between the MEN and the intermediate layer, and between the intermediate layer and the drug molecules, respectively. The field-dependent photo-absorption measurements (Figure 4) indicate the lowest and highest dissociation field strength and frequency values for GMO and EDC functionalization layers, respectively, with Tween-20 being in the middle. In fact, it should be mentioned that the complete (100%) release can be easily achieved with GMO (with field strengths of less than 100 Oe even at zero frequency), whereas only 50% release can be achieved with Tween-20 and EDC with the field strength and frequency ranges available in the current study (due to the equipment limitations). In other words, a substantially higher threshold magnetic field (>200 Oe at zero frequency) would be required to release over 50% of the PTX drug from either Tween-20-MENs or EDC-MENs. This observation correlates with the zeta-potential measurements that show the deviation of the zeta potential for the functionalized MENs from the zeta potential of the nonfunctionalized MENs. The zeta-potential values for Tween-20 and EDC-coated MENs, -34.9 ± 0.20 and -30.4 ± 0.81 mV, respectively, are higher compared with that for the nonfunctionalized MENs, -45.0 ± 1.72 mV, and GMO-coated MENs, -41.6 ± 0.26 mV. The two latter combinations require only 10-Oe and 100-Oe fields to release approximately 70% and 97% of PTX, respectively.

One side effect of the surface functionalization is the effect on the drug loading percentage and drug-binding efficacy.[35–37] It is important to consider and if possible take advantage of this effect when tailoring the properties to control the dissociation field. This effect is reflected in the current results (Figure 3). For example, the PTX loading amount is increased by over 75% and 80% after MENs are functionalized with Tween-20 and EDC, respectively, for a 3 h incubation period, compared with that for the nonfunctionalized MENs. These results are also consistent with the circulatory system-binding efficacy results, where EDC displayed over 91% drug intactness to the nanoparticles (EDC-MENs) after circulating for 2 h at 8 mL min^{-1}, which is the human coronary flow rate per minute per gram of the myocardium.[38] Finally, the in vitro cytotoxic experiment (Figure 5) indicates that neither of the nanoparticle types (MENs, GMO-MENs, of Tween-20-MENs) displays any detectable toxicity as long as the nanoparticle concentration is kept below 50 μg mL^{-1}. Moreover, GMO-MENs displays no toxicity at all (≈100% cell viability) even at the highest concentration values under study (above 100 μg mL^{-1}), indicating the true biocompatible nature of the GMO, as expected for this system.[39,40] The EDC-MENs show a slightly higher toxicity, i.e., only 77% cells were viable after 48-h treatment at 50 μg mL^{-1} concentration. By reducing the concentration of EDC-MENs to 20 μg mL^{-1}, we can increase the cell viability to over 90%. (Note: AFM analysis, mass spectroscopy analysis, and XRD analysis of the drug release process are described in the Supporting Information.)

4. Conclusions

This study focuses on the low-energy, magnetic-field-controlled release kinetics of the drug payload (popular antineoplastic drug Paclitaxel) carried by MENs. As the MEN carriers, 30-nm $CoFe_2O_4$-$BaTiO_3$ coreshell structures were used. Through a comprehensive set of experiments including FTIR, photo-absorption, XRD, AFM, zeta-potential measurements, blood circulation environment simulations, and in vitro studies on SKOV-3 cell lines, we demonstrated how the release field could be varied in relatively wide magnitude and frequency ranges, from below 10 to over 200 Oe and from 0 to over 1000 Hz, respectively, by choosing the adequate intermediate (functionalization) layer between the MEN surface and the drug molecules. Specifically, we studied the following three layer types: i) GMO (≈<10 Oe), ii) Tween-20 (≈100 Oe), and iii) EDC (>200 Oe), respectively. Using these functional layers, one could also increase the bioavailability of the drug, as they provide higher binding efficacy and thus resulting in minimal drug loss before it reaches the target. Because of the high energy efficiency of the MEN-driven delivery, MENs could also carry higher drug payloads compared with the conventional MNs and release almost 100% of the drug on demand (via application of a low-energy AC field) to the target tissue. Finally, the toxicity of the different MEN functionalization layer combinations was studied on SKOV-3 cell lines using XTT assay at the particle concentration of 50 μg mL^{-1}, which resulted in the following percentages of viable cells: i) nonfunctionalized MENs: 96%, ii) GMO-MENs: 100%, iii) Tween-20-MENs: 89%, and iv) EDC-MENs: 77%. No toxicity was observed in the case of GMO-coated MENs in the entire field strength and frequency ranges under study. In summary, these results suggest that the functionalization of MENs paves the way for a substantially broader range of applications of the new field-controlled nanocarriers (MENs) in targeted drug delivery and in medicine in general.

5. Experimental Section

MEN Fabrication: Core–shell MENs ($CoFe_2O_4$–$BaTiO_3$) were synthesized according to the method reported previously with minor modifications in the heating and cooling temperature.[41] In this method, $CoFe_2O_4$ nanoparticles were synthesized first by dissolving 0.058 g of $Co(NO_3)_2{\cdot}6H_2O$ and 0.16 g of $Fe(NO_3)_3{\cdot}9H_2O$ in 15 mL of deionized (DI) water. Later, 5 mL of aqueous solution containing 0.9 g of sodium borohydride and 0.2 g of polyvinylpyrrolidone was added at 120 °C for 12 h to obtain $CoFe_2O_4$ nanoparticles. Then, $BaTiO_3$ precursor solution was prepared by adding 30 mL of DI water containing 0.029 g of $BaCO_3$ and 0.1 g of citric acid to 30 mL ethanolic solution containing 1 g of citric acid and 0.048 mL of titanium (IV) isopropoxide. As-prepared

$CoFe_2O_4$ nanoparticles (0.1 g) were added to the 60 mL of $BaTiO_3$ precursor solution and sonicated for 120 min. The resulted dispersed nanoparticles were dried on hot plate at 60 °C for 12 h, while stirring at 200 rpm. The obtained powder was subjected to 780 °C for 5 h in a box-furnace and cooled at 52 °C min^{-1} to obtain 30 nm-sized $CoFe_2O_4$–$BaTiO_3$ coreshell MENs. The characterization data for these core–shell MENs can be found in our previous work.[21]

MEN Surface Modification: GMO-MENs were prepared by incubating 0.1 mg of GMO with 5 mg of MENs in 5 mL of PBS (pH 7.4) buffer for 12 h. (Note: to achieve uniform surface modification, the solution was slowly agitated during incubation.) The solution was later subjected to centrifugation at 20 000 rpm for 20 min at 10 °C to remove excess GMO. The obtained pellet was resuspended in ethyl acetate:acetone (70:30) solution and recentrifuged three times to obtain GMO-MENs. Tween-20-MENs were prepared by incubating 0.1 mg of Tween-20 with 5 mg of the MENs in 1 mL PBS (pH 7.4) buffer for 2 h, while agitating slowly. Later, the solution was centrifuged at 20 000 rpm for 20 min at 10 °C to remove excess Tween-20. The previous step was repeated thrice to obtain Tween-20-MENs. EDC-MENs were prepared by incubating 125 µL of EDC (conc. 1 mg mL^{-1} in PBS) with 5 mg of the MENs in 5 mL of PBS (pH 7.4) buffer for 4 h, while agitating slowly. Later, the solution was centrifuged at 20 000 rpm for 20 min at 10 °C to remove excess EDC. The previous step was repeated thrice to obtain EDC-MENs. Surface-modified MENs were lyophilized and stored at 4 °C until further use.

PTX Drug Loading: 100 µg of PTX drug was added to 1 mL methanol and PBS solution (70% methanol and 30% PBS) buffer containing 1 mg of desired nanoparticles (MENs, GMO-MENs, Tween-20-MENs, and EDC-MENs). The solution was later incubated for 3 h, while agitating slowly at room temperature. After incubation, the solution was centrifuged at 3000 rpm for 10 min at 10 °C to collect the pellet containing drug-loaded nanoparticles. The separated supernatant was isolated and measured for absorbance spectrophotometrically (Cary-100 UV–Vis) at 230 nm to determine the unbounded drug.[42] Figure S4 (Supporting Information) shows the PTX standard calibration plot obtained by varying the drug amount (50–3.25 µg) in 1 mL of PBS buffer. The drug loading percentage was calculated using Equation (1).

$$\text{Drug loading (\%)} = (\text{Total amount of drug added} - \text{Amount of drug in the supernatant}) \times 100 \quad (1)$$

Remote Magnetic Field Triggered PTX Drug Release: The isolated pellet after drug loading was washed twice with the PBS (pH 7.4) buffer to ensure the complete removal of the residual/unbounded drug. Then, the pellet was resuspended in 1 mL of PBS buffer and subjected to varying magnetic field strengths and frequencies. The magnetic fields were generated using low-powered Helmholtz coils connected to a DC power supply of 0 Hz and to an AC generator of 100 and 1000 Hz. After every single treatment, the solution was subjected to centrifugation at 3000 rpm for 3 min to separate the supernatant. This supernatant was used to measure the absorbance spectrophometrically at 230 nm to account for the amount of released drug.

SKOV-3 Cell Culture: Human ovarian carcinoma cell lines (SKOV-3) were used to investigate the in vitro cytotoxicity of the nanoparticles (MENs, GMO-MENs, Tween-20-MENs, and EDC-MENs). SKOV-3 cells were purchased from American Type Culture Collection (Manassas, Virginia). McCoy's 5A medium (Life Technologies, New York) supplemented with 10% fetal bovine serum (Sigma–Alrich) and 1% penicillin–streptomycin (science-cell) was used as a cell culture medium. SKOV-3 cells were cultured in an incubator at 37 °C temperature, 5% CO_2, and humidified atmosphere.

In Vitro Cytotoxicity Measurements: The cytotoxicity of the MENs, GMO-MENs, Tween-20-MENs, and EDC-MENs on SKOV-3 cells was measured using a quantitative colorimetric XTT (sodium 2,3,-bis(2-methoxy-4-nitro-5-sulfophenyl)-5-[(phenylamino)-carbonyl]-2H-tetrazolium inner salt) assay.[43] Approximately 0.1 million SKOV-3 cells were seeded per well in a 96-well cell culture plate along with a 100 µL of growth medium. Cell culture plate was incubated for 24 h at 37 °C to reach confluence. Then, the growth medium was replaced with the medium containing desired nanoparticles at varying concentration 0–100 µg mL^{-1} per well and allowed to incubate for another 24 h. After 24 h. incubation, growth medium containing nanoparticles was removed and cells were washed with PBS buffer twice to remove the dead cells. Now, 100 µL of the fresh medium along with a 50 µL of XTT-activated solution (from the XTT test kit supplied by ATCC) was added to each well containing the cells and was returned to the incubator for 4 more hours. (Note: XTT assay results presented were the average of three independent measurements.)

MEN Size and Surface Charge Measurements: Size and surface charge measurements of the nanoparticles were performed using Malvern Zetasizer.[44] 0.5 mg of the desired nanoparticles (MENs, GMO-MENs, Tween-20-MENs, and EDC-MENs) was dispersed in 1 mL of DI water and this solution was used to measure the size (in standard cuvette) and charge (in folded capillary cuvette). (Note: The size and charge data presented in the results are the average of three independent measurements.)

Sample Preparation for FTIR Measurements: One drop (10 µL) of the desired nanoparticle solution (MENs, GMO-MENs, Tween-20-MENs, and EDC-MENs) at concentration 1 mg mL^{-1} was taken on a pre-cleaned silicon wafer and dried over night to measure the FTIR spectrum. All the FTIR measurements were performed using JASCO-4100 instrument.

Acknowledgements

The authors acknowledge partial financial support from National Science Foundation (NSF) awards # ECCS-005084–002 and IIP-1237818, National Institutes of Health (NIH) DA # 027049, and Department of Defense (DoD) Defense Microelectronics Activity (DMEA) under contract #H94003–09–2–0904. The authors thank Luis Arroyo for his help with mass spectrometry measurements.

Received: July 10, 2013
Revised: October 8, 2013
Published online: December 9, 2013

[1] S. Douglas, S. Davis, L. Illum, *Crit. Rev. Ther. Drug Carrier Syst.* **1987**, *3*, 233.
[2] K. S. Soppimath, T. M. Aminabhavi, A. R. Kulkarni, W. E. Rudzinski, *J. Controlled Release* **2001**, *70*, 1.
[3] S. A. Agnihotri, N. N. Mallikarjuna, T. M. Aminabhavi, *J. Controlled Release* **2004**, *100*, 5.
[4] I. Slowing, B. G. Trewyn, V. S.-Y. Lin, *J. Am. Chem. Soc.* **2006**, *128*, 14792.
[5] Y. Zhang, N. Kohler, M. Zhang, *Biomaterials* **2002**, *23*, 1553.
[6] H. Gu, Z. Yang, J. Gao, C. Chang, B. Xu, *J. Am. Chem. Soc.* **2005**, *127*, 34.
[7] C. Coester, K. Langer, H. Von Briesen, J. Kreuter, *J. Microencaps.* **2000**, *17*, 187.
[8] T. Neuberger, B. Schöpf, H. Hofmann, M. Hofmann, B. von Rechenberg, *J. Magn. Magn. Mater.* **2005**, *293*, 483.
[9] A. zur Mühlen, C. Schwarz, W. Mehnert, *Eur. J. Pharm. Biopharm.* **1998**, *45*, 149.
[10] T. K. Jain, M. A. Morales, S. K. Sahoo, D. L. Leslie-Pelecky, V. Labhasetwar, *Mol. Pharm.* **2005**, *2*, 194.
[11] C.-Y. Lin, C.-J. Yu, Y.-H. Lin, W.-L. Tseng, *Anal. Chem.* **2010**, *82*, 6830.
[12] F. Dilnawaz, A. Singh, C. Mohanty, S. K. Sahoo, *Biomaterials* **2010**, *31*, 3694.
[13] M. Babic, D. Horák, M. Trchová, P. Jendelová, K. Glogarová, P. Lesný, V. Herynek, M. Hájek, E. Syková, *Bioconj. Chem.* **2008**, *19*, 740.
[14] J. R. McCarthy, R. Weissleder, *Adv. Drug Delivery Rev.* **2008**, *60*, 1241.

[15] I. P. Kaur, R. Bhandari, S. Bhandari, V. Kakkar, *J. Controlled Release* **2008**, *127*, 97.
[16] J. Homola, J. Dostálek, *Surface Plasmon Resonance Based Sensors*, Vol. *4*, Springer, Berlin, **2006**.
[17] M. J. Heffernan, N. Murthy, *Bioconj. Chem.* **2005**, *16*, 1340.
[18] I. I. Slowing, B. G. Trewyn, S. Giri, V. Y. Lin, *Adv. Funct. Mater.* **2007**, *17*, 1225.
[19] S. Sershen, S. Westcott, N. Halas, J. West, *J. Biomed. Mater. Res.* **2000**, *51*, 293.
[20] Q. A. Pankhurst, J. Connolly, S. Jones, J. Dobson, *J. Phys. D: Appl. Phys.* **2003**, *36*, R167.
[21] M. Nair, R. Guduru, P. Liang, J. Hong, V. Sagar, S. Khizroev, *Nat. Commun.* **2013**, *4*, 1707.
[22] D. Upadhyay, S. Scalia, R. Vogel, N. Wheate, R. O. Salama, P. M. Young, D. Traini, W. Chrzanowski, *Pharm. Res.* **2012**, *29*, 2456.
[23] J. Hong, E. Bekyarova, P. Liang, W. A. de Heer, R. C. Haddon, S. Khizroev, *Sci. Rep.* **2012**, *2*, 624.
[24] R. Guduru, P. Liang, C. Runowicz, M. Nair, V. Atluri, S. Khizroev, *Sci. Rep.* **2013**, *3*, 2953.
[25] D. K. Armstrong, B. Bundy, L. Wenzel, H. Q. Huang, R. Baergen, S. Lele, L. J. Copeland, J. L. Walker, R. A. Burger, *New Engl. J. Med.* **2006**, *354*, 34.
[26] A. Sunters, S. F. de Mattos, M. Stahl, J. J. Brosens, G. Zoumpoulidou, C. A. Saunders, P. J. Coffer, R. H. Medema, R. C. Coombes, E. W.-F. Lam, *J. Biol. Chem.* **2003**, *278*, 49795.
[27] E. E. Vokes, K. Stenson, F. R. Rosen, M. S. Kies, A. W. Rademaker, M. E. Witt, B. E. Brockstein, M. A. List, B. B. Fung, L. Portugal, *J. Clin. Oncol.* **2003**, *21*, 320.
[28] R. Mahajan, K. Patankar, M. Kothale, S. Chaudhari, V. Mathe, S. Patil, *Prama* **2002**, *58*, 1115.
[29] Y. Zhang, C. Deng, J. Ma, Y. Lin, C.-W. Nan, *Appl. Phys. Lett.* **2008**, *92*, 062911.
[30] K. Matsuzaki, M. Harada, S. Funakoshi, N. Fujii, K. Miyajima, *Biochim. Biophys. Acta Biomembranes* **1991**, *1063*, 162.
[31] A. Borges, P. Bourban, J. Månson, *ICCM-17 Proceedings*, **2009**, D2, Edinburgh, UK.
[32] X. Li, Y. He, M. T. Swihart, *Langmuir* **2004**, *20*, 4720.
[33] L. Zhu, J. Ma, N. Jia, Y. Zhao, H. Shen, *Colloids Surf. B. Biointerfaces* **2009**, *68*, 1.
[34] J. S. Kim, T.-J. Yoon, K. N. Yu, B. G. Kim, S. J. Park, H. W. Kim, K. H. Lee, S. B. Park, J.-K. Lee, M. H. Cho, *Toxicol. Sci.* **2006**, *89*, 338.
[35] E. Acosta, *Curr. Opin. Colloid Interface Sci.* **2009**, *14*, 3.
[36] V. Labhasetwar, C. Song, W. Humphrey, R. Shebuski, R. J. Levy, *J. Pharm. Sci.* **1998**, *87*, 1229.
[37] R. P. Bagwe, L. R. Hilliard, W. Tan, *Langmuir* **2006**, *22*, 4357.
[38] D. J. Duncker, R. J. Bache, *Physiol. Rev.* **2008**, *88*, 1009.
[39] J. Reeff, A. Gaignaux, J. Goole, J. Siepmann, F. Siepmann, C. Jerome, J. Thomassin, C. De Vriese, K. Amighi, *Int. J. Pharm.* **2013**,*451*, 95.
[40] M. H. Shah, S. V. Biradar, A. R. Paradkar, *Int. J. Pharm.* **2006**, *323*, 18.
[41] V. Corral-Flores, D. Bueno-Baques, R. Ziolo, *Acta Mater.* **2010**, *58*, 764.
[42] W. Geldenhuys, T. Mbimba, T. Bui, K. Harrison, V. Sutariya, *J. Drug Targeting* **2011**, *19*, 837.
[43] N. W. Roehm, G. H. Rodgers, S. M. Hatfield, A. L. Glasebrook, *J. Immunol. Methods* **1991**, *142*, 257.
[44] R. A. Alvarez-Puebla, E. Arceo, P. J. Goulet, J. J. Garrido, R. F. Aroca, *J. Phys. Chem. B* **2005**, *109*, 3787.